Talanta 249 (2022) 123625

Contents lists available at ScienceDirect

Talanta

journal homepage: www.elsevier.com/locate/talanta

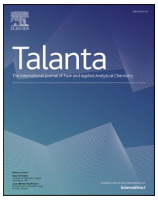

# Development of a microfluidic droplet platform with an antibody-free magnetic-bead-based strategy for high through-put and efficient EVs isolation

Marco Morani [a], Myriam Taverna [a,b], Zuzana Krupova [c], Lucile Alexandre [a,d], Pierre Defrenaix [c], Thanh Duc Mai [a,*]

[a] Université Paris-Saclay, CNRS, Institut Galien Paris-Saclay, 92296, Châtenay-Malabry, France
[b] Institut Universitaire de France (IUF), France
[c] Excilone - 6, Rue Blaise Pascal - Parc Euclide, 78990, Elancourt, France
[d] Laboratoire Physico Chimie Curie, Institut Curie, PSL Research University, CNRS UMR168, Paris, France

ARTICLE INFO

*Keywords:*
Extracellular vesicles
Isolation
Magnetic beads
Polymer precipitation
Microfluidic droplets

ABSTRACT

In this study, we present a novel microfluidic droplet-based strategy for high performance isolation of extracellular vesicles (EVs). For EVs capture and release, a magnetic bead-based approach without having recourse to any antibody was optimized in batch and then adapted to the microfluidic droplet system. This antibody-free capture approach relies on the presence of a water-excluding polymer, polyethylene glycol (PEG), to precipitate EVs on the surface of negatively charged magnetic beads. We significantly improved the reproducibility of EV recovery and avoided positive false bias by including a washing step and optimizing the protocol. Well-characterized EV standards derived from pre-purified bovine milk were used for EVs isolation performance evaluation. An EVs recovery of up to 25% estimated with nanoparticle tracking analysis (NTA) was achieved for this batchwise PEG-based approach. The confirmation of isolated EVs identity was also made with our recently developed method using capillary electrophoresis (CE) coupled with laser-induced fluorescent (LIF) detection. In parallel, a purpose-made droplet platform working with magnetic tweezers was developed for translation of this PEG-based method into a droplet microfluidic protocol to further improve the performance in terms of EVs capture efficiency and high throughput. The droplet-based protocol offers a significant improvement of recovery rate (up to 50%) while reducing sample and reagent volumes (by more than 10 folds) and operation time (by 3 folds) compared to the batch-wise mode.

## 1. Introduction

Extracellular vesicles (EVs) are phospholipid bilayer-delimited particles produced by most cell types and present in many body fluids [1,2]. EVs contain and carry diverse biomolecules that are specific to the mother cells from which they are secreted, allowing them to transmit a variety of essential signals under both normal and pathological conditions. Hence, the potential of EVs as prognostic or diagnostic biomarkers has attracted significant attention in recent years [3,4]. Furthermore, due to their high specific targeting ability, EVs have gained much interest as engineered drug delivery systems for clinical and pharmaceutical applications [5,6]. However, there are still technological hurdles to purify, analyze and characterize such nanometric bio-entities. Many methods for isolating EVs have been developed so far, including ultracentrifugation (UC), gradient ultracentrifugation, ultrafiltration (UF), polymer co-precipitation, size-exclusion liquid chromatography (SEC), immuno-extraction [7]. Among these, ultracentrifugation is widely considered as the gold standard in all EV applications. However, this technique presents many drawbacks, such as time-consuming procedures, contamination of EV populations by protein aggregates and other particles, damage to the EVs membrane structure and possible considerable loss of EVs (EVs yield may drop to 2%) [8,9]. Thus, there is still an urgent need for emerging EVs isolation approaches that can provide EV purity and integrity in a reproducible and high-throughput manner. Many modern isolation methods have been developed in this direction, such as flow field-flow fractionation, ion-exchange, electrokinetic

* Corresponding author.
*E-mail address:* thanh-duc.mai@universite-paris-saclay.fr (T.D. Mai).

https://doi.org/10.1016/j.talanta.2022.123625
Received 20 January 2022; Received in revised form 25 May 2022; Accepted 26 May 2022
Available online 30 May 2022

approaches as well as the combination of multiple techniques, like UC with UF or SEC [10–12]. In parallel, microfluidic technologies have made significant progresses for such purpose, exploiting both physical and biochemical properties of EVs at micro/nanoscale level for their capture and/or detection [13–17]. The majority of microfluidic approaches rely on immunoaffinity to selectively capture EVs. Immunoaffinity bead-based kits allow highly selective isolation of EVs through antibodies specific for target EVs surface proteins [18–20]. However, following isolation, those commercial kits, which are rather used for subsequent EVs downstream lysis and analysis, do not provide any efficient elution possibility to recover intact EVs. Moreover, the main disadvantage of those strategies is the absence of universal EVs markers to ensure total capture of all EVs. Few recent works on capture and eventual elution of EVs on magnetic beads have been reported, using either electrostatic interaction [21], polymer mediated adsorption of EVs on magnetic beads [22], a DNA aptamer-based system [23] or DNA linker spacers [24]. No EVs recovery efficiency was reported in these works that used cell culture media and/or plasma samples as starting materials from which accurate EVs quantification is not trivial. At the actual stage, these works had to be realized batchwise with multiple in-tube steps without automation.

The goal of this study was to investigate bead-based strategies for isolating and recovering intact EVs without the use of immunoaffinity recognition and to adapt them to droplet microfluidics. For such purposes, well-characterized high-quality EVs isolated from bovine milk were used as EVs standards rather than non-quantified EVs from cell culture and plasma samples. Then, the batchwise approach with the superior performance was transferred into an automated and high-throughput protocol relying on a microfluidic droplet train. Different operations in microfluidic droplets were developed and optimized to overcome the challenges of beads clustering and poor recirculation in droplets in the presence of viscous polymers, allowing to realise EVs capture on beads, washing and elution with a droplet sequence. So far, droplet microfluidics has been communicated only twice for immunoassay-based detection of EVs [25,26] and has never been exploited for high performance and high throughput isolation of EVs.

## 2. Materials and methods

### 2.1. Chemicals and reagents

2-(cyclohexylamino)ethanesulfonic acid (CHES), phosphate buffered saline (PBS 10x), sodium dodecyl sulfate (SDS, 98.5% (GC)), tris (hydroxymethyl)aminomethane (Tris), polyethylene glycol (PEG 8000), albumin from human serum, IgG from human serum and human transferrin were all obtained from Sigma Aldrich (St. Louis, MO, USA). Sodium hydroxide (1 M) and hydrochloric acid (1 M) were obtained from VWR (Fontenay-sous-Bois, France). All solutions were prepared with deionized water purified with a Direct - Q3 UV purification system (Millipore, Milford, MA, USA). Vybrant™ CFDA SE Cell Tracer Kit (dye 5-(and-6)-carboxyfluorescein diacetate succinimidyl ester, CFDA-SE) was purchased from Thermo Fisher Scientific (Waltham, MA, USA). Fluorinert oil FC-40 (ZF-0002-1308-0) was purchased from 3 M (USA). The surfactant 1H, 1H, 2H, 2H – perfluoro-1-decanol was obtained from Sigma Aldrich. ExoCAS-2 kit containing poly-L-lysine-coated magnetic beads, washing and elution buffer solutions was purchased from Microgentas (Seongbuk-gu, Republic of Korea). Carboxylate functionalized magnetic beads (Dynabeads MyOne, 10 mg/mL, diameter of 1 μm) and silica-based magnetic beads (Dynabeads MyOne Silane, 40 mg/mL, diameter of 1 μm) were obtained from Thermo Fisher Scientific. EVs samples isolated from bovine milk were provided by Excilone (Elancourt, France).

### 2.2. Apparatus and material

For macroscale protocols, all magnetic-bead-based assays in batch were carried out in protein LoBind 1.5 mL tubes purchased from Eppendorf (Hamburg, Germany). For retaining magnetic beads, a neodymium magnet purchased from Ademtech (Adem Mag MSV, Bessac, France) was used. Shaking of magnetic bead suspensions during the incubation and washing steps was realized with a mixer (Eppendorf ThermoMixer C).

For droplet microfluidic operations, a microfluidic droplet platform was constructed and was inspired from our previous configuration [27]. It comprises a syringe pump (from Nemesys, Cetoni GmbH) equipped with 1 mL glass syringes (purchased from SGE) and a motorized pipettor arm (Rotaxys, Cetoni GmbH), used for droplets generation. A 96-well plate (Thermo Scientific) was used for sample storage and reagent solutions. The plate was mounted on a custom-made holder that can be moved in the X, Y, and Z directions. PTFE tubing with ID of 0.3 mm and OD of 0.6 mm (Z609692-1PAK, Sigma Aldrich) was used to conduct the droplet trains. Fluorinated oil FC-40 mixed with the surfactant (1H, 1H, 2H, 2H − perfluoro-1-decanol, 2% w/w) was used to separate aqueous droplets inside PTFE tubing. In the protocol, a magnetic tweezer, prepared in-house was used. It is composed of a paramagnetic tip activated by a magnetic coil. Macro Objective (MLH-10X) mounted on a low-cost CMOS Cameras (acA1300-60 gm, Basler) and white LED back light illumination (Schott Lighting and Imaging) were employed for droplet observation.

The analyses using CE coupled with laser induced fluorescent detection (CE-LIF) were performed with a PA 800 Plus system (Sciex Separation, Brea, CA) equipped with a solid-state LIF detector (excitation wavelength of 488 nm, emission wavelength of 520 nm) purchased from Integrated Optics (Art. No. 40A-48A-52A-64A-14-DM-PT, distributed by Acal BFi, Evry, France). Uncoated fused silica capillaries were purchased from CM Scientific (Silsden,UK). Data acquisition and instrument control were carried out using Karat 8.0 software (Sciex Separation, Brea, CA).

### 2.3. Methods

#### 2.3.1. Isolation of bovine milk-derived EVs with sucrose gradient ultracentrifugation

Skimmed bovine milk samples were obtained by centrifugation of 50 mL whole milk at 3000 g for 30 min at 4 °C (Allegra X-15R, Beckman Coulter, France).The whey was obtained after acid precipitation with 10% (v/v) acetic acid, incubation at 37 °C for 10 min and 10% (v/v) 1 M sodium acetate for 10 min at RT followed by centrifugation at 1500*g*, 4 °C for 15 min and filtration using vacuum-driven filtration system Millipore Steritop, 0.22 μm. The whey supernatants were concentrated using Amicon 100 kDa centrifugal filter units (Merck Millipore) at 4000 g and 20 °C up to final volume of 6 mL. The obtained retentate was ultracentrifuged for pelleting the EVs at 100000 g for 70 min at 4 °C (Beckman Coulter, Optima XPN-80, 50TI rotor). The pellets were solubilized in 500 μL of PBS then added to 11 mL of pre-prepared sucrose gradient 5–40% and ultra-centrifuged at 200000 g for 18 h at 4 °C (Beckman Coulter, Optima XPN-80, SW41 rotor). Fractions of 1 mL were collected and the selected ones containing targeted exosome population were diluted in 6 mL of PBS 1X and finally centrifuged at 100000 g for 70 min at 4 °C (Beckman Coulter, Optima XPN-80, 50TI rotor). The pellets were resuspended in 50 μL of PBS 1X and stored at −80 °C, until further analyses.

Isolation of pony plasma and serum derived EVs with size exclusion chromatography (SEC).

Preparation of plasma: Peripheral blood was collected into EDTA-coated vacutainer tubes. After ten-time inversion, samples were processed within the 60 min of collection. Consecutive centrifugation steps at 2500 g, 4 °C for 15 min and then at 15000 g for 10 min were performed followed by filtration of the supernatant through 0.22 μm filters. Preparation of serum: Whole blood was collected into anticoagulant-free tubes and allowed to clot at room temperature for 45 min. The clot was removed by centrifugation at 3200*g*, 4 °C for 15 min, followed by

centrifugation at 15000*g*, 4 °C for 10 min and filtration of the supernatant through 0.22 μm filters. 500 μL of pre-treated plasma/serum was loaded onto a qEVoriginal SEC column (Izon Science, New Zealand) previously washed and equilibrated with PBS. Fraction collection (0.5 mL per fraction) was carried out immediately using PBS 1X as elution buffer. The selected elution fractions were pooled and subsequently concentrated using 100 kDa Amicon centrifugal filter units (Merck Millipore). Post-treatment processing with several washing steps with PBS was applied to obtain pure EV fractions that are highly enriched with exosomes.

### 2.4. EV isolation using commercial kits

ExoCAS-2 magnetic bead-based ion exchange kit was used for the study of EV yield performance. The experimental procedure is described in a paper recently published [21]. Briefly, PLL-coated beads were mixed with our standard EVs (bovine milk derived EVs), followed by incubation of the mixture for 30 min at 4 °C in a rocking mixer. After incubation, the EVs-bound beads were carefully washed with 2 mL of ExoCAS-2 washing solution and then re-suspended in ExoCAS-2 elution solution by shaking for 5 min at 1000 rpm. Finally, a magnet was employed to retain magnetic beads and the supernatant containing yielded EVs was collected.

### 2.5. PEG-based EVs precipitation on magnetic beads in batch mode

For PEG-based EVs precipitation on magnetic beads in batch, a volume of 200 μL of PEG (25% m/v), 150 μL of carboxylate functionalized magnetic beads (10 mg/mL) and 250 μL of deionized water was incubated with 400 μL of standard EVs or biological fluid (simulated human serum and pony plasma and serum, 5 times diluted with deionized water) on a mixer at 25 °C for 1 h at 700 rpm. Beads were then carefully washed twice with PEG 5%/NaCl 0.2 M. After removal of washing solution, the magnetic beads in tubes were re-dispersed in 400 μL of PBS 1X solution and then incubated on shaking for 5 min at 25 °C for EV elution. A magnet was used to remove the magnetic beads, and EVs were recovered in the supernatant.

PEG-based EVs precipitation on magnetic beads using the microfluidic droplet platform.

A robotic arm and a 500 μL syringe were utilized to pipette the droplets from separate reservoirs into a PTFE tube in a fully automated manner. To complete one PEG-based EVs precipitation protocol, a train of 5 droplets (each containing 6 μL) confined and separated by oil was required. It includes: i) one droplet of carboxylate functionalized magnetic beads (1.5 mg/mL), ii) one droplet of EV sample in PEG 5%, iii-iv) two droplets of washing solution (PEG 5%/NaCl 0.2 M) and v) one droplet of elution solution (PBS 1X). Beads were trapped out of one droplet and released into another by electronic triggering of the magnetic tweezer. The incubation was carried out with regular droplet back and forth movements at RT for 25 min. After incubation, two washing droplets are flushed over EVs-bound beads. The EVs-bound beads were then dispersed into the elution droplet with regular droplet back and forth movements at RT for 5 min. The elution droplet containing released EVs was then collected in a tube for downstream analysis.

### 2.6. Nanoparticle tracking analysis (NTA) of EVs

Particle concentration and size distribution were determined with a Nanosight NS300 instrument (Malvern, version NTA 3.2 Dev Build 3.2.16) equipped with a 405 nm laser, sCMOS camera type and the NTA software v3.1. The video acquisition was performed using a camera level of 14. 3 videos of 90 s with a frame rate of 30 frames/s were captured for each sample at 25 °C and subsequently analyzed with a threshold set up at 5. The results were validated with at least 2000 valid tracks for each triplicate. All experiments were carried out with samples pre-diluted in PBS according to input sample concentrations. The working particle concentrations were kept within the range of $10^6$ - $10^9$ particles per mL for optimal analysis.

The Zetaview system (Particle Metrix, Germany) was equipped with a 488 nm laser. EVs samples were diluted to allow the measurements at 50–200 particles/frame. Each experiment was performed in duplicate on 11 different positions within the sample cell. The specifications used for all measurements were cell temperature of 25 °C, sensitivity of 70, shutter of 100, Max Area of 1000, Min Area of 10, Min Brightness of 25. The results were validated with at least 1000 valid tracks for each run. For data capture and analysis, the Nanoparticle Tracking Analysis Software (ZNTA) vs 8.05.04 was used.

### 2.7. CE-LIF of fluorescently labelled EVs

Details on the CE-LIF method for EVs analysis can be seen in our recent work [28]. Briefly, fluorescently labelled EVs were prepared using the 5-(and-6)-carboxyfluorescein diacetate succinimidyl ester (CFDA-SE). After removal of residual CFDA-SE via filtration with commercial Exosome Spin Columns (MW 3000, Thermo Fisher Scientific Waltham, MA USA), labelled EVs were analyzed with CE-LIF using a fused silica capillary having I.D. of 50 μm, effective length ($L_{eff}$) of 50.2 cm and total length ($L_{tot}$) of 60.2 cm. The capillary was pre-conditioned with water for 10 min, 1 M NaOH for 10 min, 1 M HCl for 10 min and then water for 10 min. The rinsing between two analyses was carried out with 50 mM SDS for 5 min, 1 M NaOH for 5 min, deionized water for 5 min, and finally the running BGE composed of Tris/CHES (IS 90 mM, pH 8.4) for 5 min using a pressure of 30 psi. EVs samples were injected hydrodynamically from the inlet end by applying a pressure of 0.5 psi for 2 min. The separation was carried out under 25 kV (normal polarity) at 25 °C and the samples were kept at 5 °C with the sample storage module of the PA 800 Plus equipment.

## 3. Results and discussion

### 3.1. Batchwise EVs isolation development

With the aim to establish a high-performance and high-throughput microfluidic droplet system for EVs isolation, we evaluated two recently communicated batchwise EV-enrichment strategies that are alternative approaches to the immunoaffinity-based ones. They hold high potential for subsequent translation into a microfluidic format in terms of minimal forefront preparations, non-laborious operations, as well as ease of manipulation and step transition thanks to the use of magnetic beads as cargos. The first one is a magnetic bead-mediated selective adsorption strategy (MagExo), exploiting the presence of a water-excluding polymer, polyethylene glycol (PEG), to lock up a significant number of water molecules, forcing thereby the EVs to aggregate and precipitate on the surface of magnetic beads [22]. The second strategy called ExoCAS-2 relies on an ionic exchange mechanism, using magnetic beads coated with a polycationic polymer, poly-L-lysine (PLL), to quickly trap negatively charged EVs via electrostatic interaction [21]. For performance comparison, EVs standards derived from bovine milk having narrow size distribution, with well-defined concentrations and exhaustive characterizations by NTA, DLS, LC-MS/MS and TEM, were used as the starting sample. TEM images revealed the absence of contaminating protein residues in these EVs standards (Fig. S1A in the supporting information ESI). Major protein contaminants (e.g. α-s1 casein, β-casein, α-Lactalbumin and serum albumin) were not found according to the LC-MS/MS analysis (Fig. S1B). The use of EV standards of high purity allowed to evaluate the EVs recovery more accurately. In our case, quantification of EVs isolation yields obtained with MagExo and ExoCAS-2 methods was possible by comparing the EVs concentrations before and after isolation processes (see Fig. 1). Unsatisfactory EVs recovery (less than 10%) was obtained with commercial PLL-coated beads, compared to that achieved when using PEG and silica magnetic beads (34%). NTA data also showed a size shift towards smaller particles

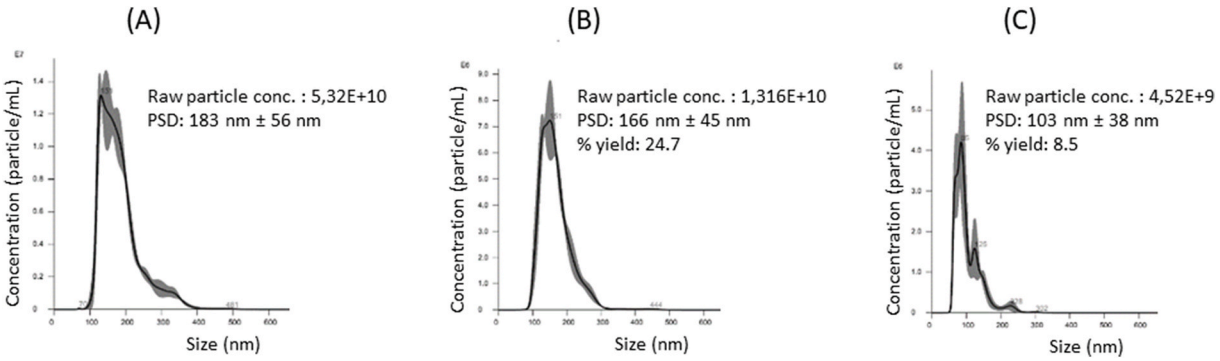


**Fig. 1.** NTA measurements of EVs isolated from bovine milk before purification (A) and after purification with (B) MagExo or (C) ExoCAS-2 method. NTA histograms represent the mean of three replicate measurements of the same sample, with the standard deviation (SD) in grey.

when EVs were eluted from PLL beads. This could be a consequence of PLL release from the beads during the elution process. This was confirmed by the CE-LIF analysis (discussion below). This led to a critical PLL concentration in the eluent that is high enough to cause EVs lysis. Indeed, several studies have shown that PLL can penetrate through vesicles via interaction with the lipid membrane [29–31], provoking vesicle lysis from a certain threshold concentration of PLL [32]. In parallel to NTA measurements for EVs recovery evaluation, we used our recently developed CE-LIF approach [28] to validate the identity of EVs collected with MagExo and ExoCAS-2 methods (see Fig. 2). The peak profile of EVs collected with PEG-based protocol corresponds well to the fingerprint of bovine milk-derived EVs, confirming the presence of intact EVs in the eluent (Fig. 2A). On the contrary, with the ion exchange method, multiple tagged species were detected. To understand the origin of these peaks, solutions containing different PLL concentrations without the presence of EVs were analyzed. As can be seen in Fig. 2B, many peaks were still detected, whose intensities were related to the PLL concentrations. These results confirmed the hypotheses that the peaks observed come from PLL leakage from the magnetic beads, which could not be visualized with conventional NTA. The released PLL which can be labelled by the residual CFDA-SE dye through its amino groups lead to unwanted products in the eluent. The ExoCAS-2 method was therefore not further considered; and the PEG-based method (MagExo) was chosen for further optimization.

Besides the preservation of intact EVs after purification, protocol reproducibility is another important point to consider to guarantee consistency of isolated EVs population and quality. Indeed, by reproducing the MagExo procedure described in Ref. [22], we observed significant batch-to-batch variation in vesicle concentration (RSD of 30%). The lack of EVs washing between the capture and elution steps in the original protocol led to misleading data. To minimize this cross contamination and to recover intact EVs for further characterization, we developed a washing protocol after the EVs capture step. By adding two consecutive washing steps with PEG 5% w/v to remove residual unbound EVs while maintaining captured EVs on magnetic beads, we significantly improved the repeatability (RSD) to 8%. This came with some penalty, as the EV isolation yield fell to 17%. To further improve the performance of EVs capture and thus isolation yield, we carried out different optimizations on magnetic bead concentrations (0.5–2 mg/mL), bead chemical surface (with carboxylic or silane groups), incubation temperature for EVs capture (4–25 °C) as well as PEG concentrations (5–15% w/v). Note again that the performance of EVs capture relies on the presence of PEG to force the EVs to precipitate (by locking up a significant number of water molecules) on the surface of magnetic beads. As can been seen in Fig. S2 in the ESI, much better EVs capture performance was achieved with beads with carboxylic groups (EVs yield of 61%) than with silane groups (less than 5%). The incubation temperature was found not to significantly influence the EVs capture performance, with no remarquable difference observed at 4 °C (yield of 17.2%) and 25 °C (yield of 20%). The concentrations of magnetic beads and PEG played important roles in the on-bead retaining of EVs. A compromise of their concentrations had to be made to allow facile PEG-induced precipitation of EVs on sufficient quantity of carboxylate beads, while avoiding i) poor recirculation or even clustering of beads at too high concentrations and ii) hindrance of the arrival of EVs on to the beads surface due to too elevated medium's viscosity at too high PEG concentrations. Overall, the highest EVs recovery rate (after 2 washing steps) of 25% ± 8% was achieved with the optimized conditions using PEG concentration of 5% and carboxylic magnetic beads' concentration of 1.5 mg/mL with 1 h incubation at 25 °C. A higher bead concentration of 2 mg/mL was tested but no satisfactory results were obtained due to clustering and poor circulation of beads. PEG concentrations lower than 5% w/v were not considered in our work, based on previous optimization already reported [22]. Conveniently, the working temperature of 25 °C is well adapted for subsequent translation of batchwise protocol into a microfluidic format where cooling function is not readily available. To evaluate the reusability of magnetic beads functionalized with carboxylic groups for repeated isolation of EVs, the same beads employed for the first round of capture and elution of EVs were recovered in PBS and then subjected to the second and third rounds. As shown in Fig. S3 in the ESI, the concentration range of recovered EVs in the second round is similar to that obtained from the first round. The variation of recovered EVs concentrations is however significantly higher (RSD of 24% vs. 9%, respectively). While the surface charge of the beads is expected not to be hammered by the elution media (i.e., PBS), the possible presence of residual PEG on the surface of beads after the first elution step could explain such an elevated variation in the second round. When using the same beads for the third cycle of EVs capture – elution, no satisfactory results were obtained, with the recovered EVs concentration almost 5-fold lower than those obtained in previous cycles (Fig. S3 in ESI). While the reusability of magnetic beads for EVs capture and elution is possible for 2 cycles with careful consideration of PEG presence, fresh beads without recycling are nevertheless required for further experiments in order to minimize the risk of EVs isolation uncertainty.

### 3.2. *Droplet microfluidics for EVs isolation: proof of concept*

The optimized batchwise PEG-based method was subsequently converted into a microfluidic droplet protocol in order to provide a high level of automation and integration, significant reduction in sample/reagent amounts, and a higher performance in terms of isolation efficiency. The instrumental setup of the purpose-made microfluidic platform is shown in Fig. 3. It is composed of a syringe pump, a motorized pipettor arm for droplet production, a 96-well plate for sample and reagent storage and a magnetic tweezer for manipulation of magnetic beads. With this system, we used a train of 6 μL droplets containing in a defined sequence (i) the magnetic bead suspension, (ii) the EVs sample,

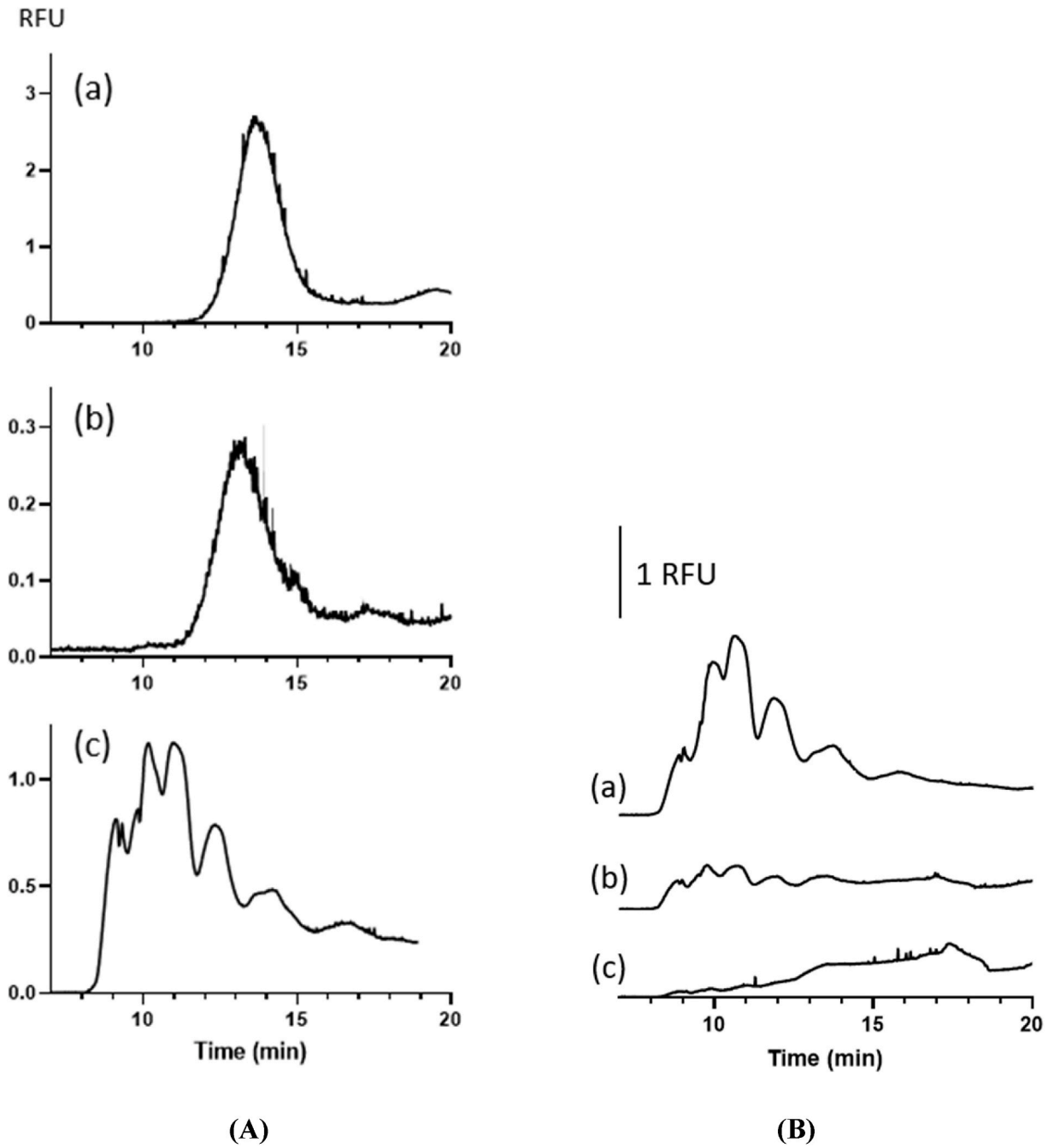


**Fig. 2.** (A) CE-LIF measurements of EVs before purification (a), and after purification with (b) MagExo or (c) ExoCAS-2 method. (B) CE-LIF profiles of solutions of PLL at different concentrations, corresponding to PLL-coated beads suspension volumes of (a) 1 mL; (b) 0.5 mL; (c) 0.1 mL. CE-LIF conditions: fused silica capillary having I.D. of 50 μm, effective length ($L_{eff}$) of 50.2 cm and total length ($L_{tot}$) of 60.2 cm; BGE composed of Tris/CHES (IS 90 mM, pH 8.4); applied voltage: 25 kV (normal polarity).

(iii) the washing and (iv) elution solutions to replace different tube-based steps. When working with the droplet-wise multi-step protocol, one hurdle encountered is the difficulty to efficiently transfer the target species (EVs in this case) from one droplet to another without any risk of cross contamination. This was expected to be overcome with our setup through the use of magnetic beads as the controllable carrier of target analytes between droplets. A purpose-made magnetic tweezer, composed of a paramagnetic tip activated by an electrical coil [27,33], was employed to manipulate magnetic beads between droplets via application of an external electrical field. Table 1 provides an overview of the operation sequence. A train of droplets containing different solutions and sample in a defined order was delivered through the magnetic tweezer where the beads were extracted from the first droplet and transported into the sample one containing EVs. The incubation was subsequently performed by pushing the droplet train back and forth inside the tubing. The magnetic beads that retain EVs on their surface were then trapped by the magnetic tweezer and the supernatant droplet was washed away, followed by flushing of the trapped magnetic beads with two washing droplets. The washed beads were finally released into an elution droplet that was finally collected in an oil-containing tube for further analyses.

Several problems were however encountered that led to failure of such droplet protocol in our first experiments, notably beads clustering and poor recirculation in droplets in the presence of PEG. Indeed, the

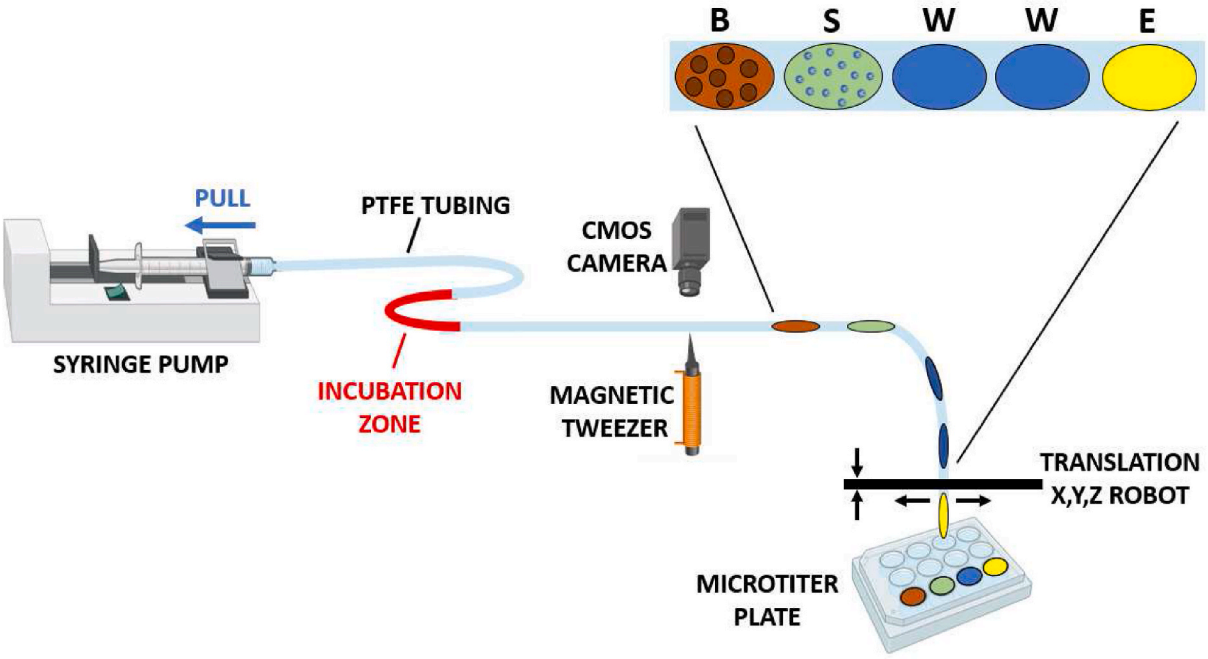


**Fig. 3.** Schematic drawing of microfluidic droplet system. B: droplet containing magnetic beads; S: sample droplet; W: washing droplet; E: droplet containing the elution solution. Droplets are separated by oil.

**Table 1**
Operation sequence of the microfluidic droplet protocol using droplets of 6 μL each.

| Operation | Droplet composition | Flowrate (μL/s) | Incubation time (min) | Back-and-forth droplet travel distance (+/− μL) |
|---|---|---|---|---|
| Sample incubation | EVs sample + PEG 5% (w/v) + magnetic beads (1.5 mg/mL | 4 | 25 | 6 |
| Washing 1 | PEG 5%/NaCl 0.2 M | 0.5 | Flush | – |
| Washing 2 | PEG 5%/NaCl 0.2 M | 0.5 | Flush | – |
| Sample elution | PBS 1X | 4 | 5 | 6 |

beads often stayed at the rear of the moving droplet, forming undesired bead clusters when the droplet moved inside the tubing over an extended distance. This was ascribed to come from the presence of PEG which significantly increased droplet viscosity [34], which in turn impaired the effective recirculation of the beads (see Fig. S4 in the ESI). To enhance recirculation of the beads within a droplet, we put our efforts on optimizing the droplet movement pattern and travel volume (i.e., the oil volume required to push and pull the droplet) during the back-and-forth movement. Chaotic trajectories are known to enhance mixing efficiency [35,36]. Consequently, different droplet movement patterns were also tested, including the straight, the U-shaped patterns (i.e., the tubing was shaped over a metallic guideline) and the spiral-formed one (i.e., the tubing was coiled around a cylindrical support) (see Fig. S5 in ESI). With the straight pattern, bead aggregation was always observed in the presence of PEG, regardless of the travel volume (Fig. S4A). For other movement patterns, bead clustering was alleviated but still visible when working with a large travel volume of 10 μL (Fig. S4 B and C). This undesired phenomenon was finally avoided when employing the spiral or U-shaped patterns with a short travel volume of 6 μL (equivalent to a droplet volume). By keeping these optimized setups and conditions, we further investigated the in-droplet incubation duration (from 5 to 45 min) during the EVs capture step (Fig. S6 in the ESI). The EVs recovery increased from 10% for 5 min incubation to 27% for 25 min incubation, and remained stable even when the incubation time was increased up to 45 min . For the spiral-formed pattern, the best EVs recovery of 27% ± 4% was thus found for 25 min incubation Under the same incubation time, the U-shaped pattern offered the EVs recovery rate of 39% ± 3%, indicating better interaction between EVs and magnetic beads, and thus higher EVs capture efficiency for the U-shaped pattern. Among the tested droplet movement ones, the straight one gave the least EVs recovery (14% ± 4%) and therefore was not further considered. To obtain more precise information on the quality of the isolated EVs, the samples were analyzed with Particle Metrix' ZetaView [37]. As revealed by Zetaview data (Fig. 4B), 80% of the recovered EVs fell within the range of the initial size distribution (diameter of 171 nm, accounting for 79% of the whole population), while the remaining 20% were represented by larger aggregates (16.7% for the diameter of 315 nm, and 4.3% for 472 nm). These aggregates are presumably formed due to the PEG capacity to wrap and condense together two or three EVs (corresponding to the sizes of 317 and 472 nm, respectively), making them hard to resuspend in the absence of PEG during the elution step.

### 3.3. Microfluidic droplet-based isolation of EVs from biofluids

The developed microfluidic droplet instrument and protocol were then used to isolate EVs from more complex matrices. First, we used PBS mixed with three matrix proteins, including albumin, IgG and transferrin to imitate human extracellular fluids [38]. This simulated human serum was then spiked with standard EVs (*i.e.*, bovine milk derived EVs at $1.02 \times 10^{11}$ particles/mL) and passed through the microfluidic droplet system to evaluate the EVs isolation performance. As indicated in Fig. 5, the concentration of collected EVs was $3.69 \times 10^{10}$ particles/mL, giving an EVs recovery rate of 36% with spiked simulated human serum, which was not far from that obtained with pure standard EVs (39%). We then applied the droplet protocol to pony plasma and serum, and compared the results obtained with the in-tube batchwise protocol (Fig. S7 in ESI). When dealing with such complex biofluid

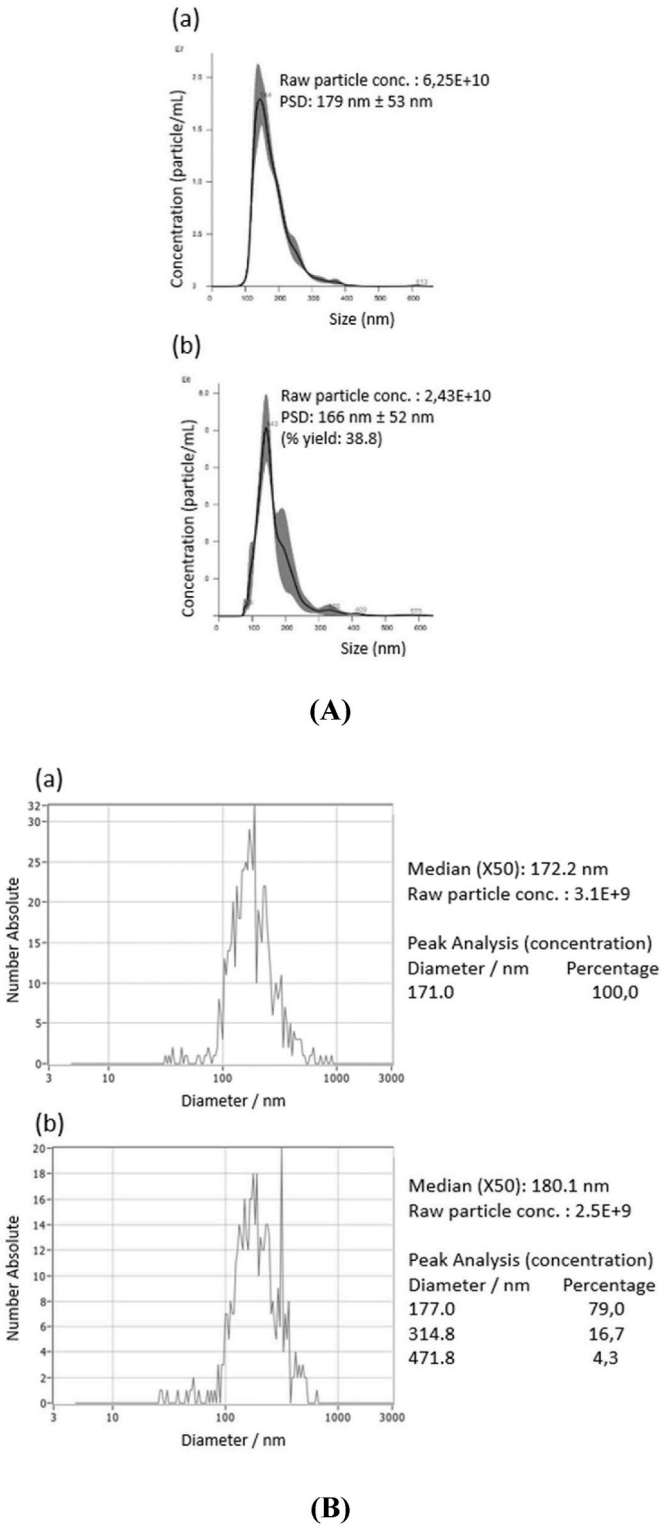


**Fig. 4.** Comparison between (A) Nanosight NS300 (Malvern) *vs* (B) Zetaview NTA (Particle Metrix) for EVs standard before (a) and after (b) purification with the microfluidic droplet platform using the U-shaped pattern. NTA histograms represent the mean of three replicate measurements of the same sample, with the standard deviation (SD) in grey.

matrices, the droplet approach gave an overall particle concentration much higher (up to eight folds) than those obtained with the in-tube method. For instance, with the pony serum sample, the recovered EVs concentration was $8 \times 10^{10}$ particles/mL when using the microfluidic droplet platform, whereas a significantly lower one ($1.05 \times 10^{10}$ particles/mL) was found for the in-tube method. A similar observation was found for pony plasma, with $17.7 \times 10^{10}$ particles/mL vs. $4.9 \times 10^{10}$ particles/mL for microfluidic and in-tube setups, respectively. Moreover, the size distributions of EVs purified with the microfluidic droplet setup are much narrower with only one main peak for each tested sample (Fig. S7). This was, on the other hand, not the case for the in-tube protocol where many peaks were found in the range of 70–400 nm for both pony serum and plasma samples. To confirm the identity of EVs isolated from plasma and serum samples, the elution droplets were also analyzed with CE-LIF to reveal different EVs subpopulations (Fig. 6). Based on the peak intensities in each electropherogram, the highest concentration was found for the fraction with the shortest migration time (9–12 min) whereas the signal of the second peak zone (12–15 min) was less intense and this is more remarked for the serum samples. This kind of EVs fingerprints was found similar to those obtained in our previous work with EVs from pony plasma and serum isolated by SEC [28]. Interestingly, the third peak zone (15–20 min) appeared in the electropherograms obtained with both in-batch mode and the droplet system, suggesting that a distinct subpopulation emerges when using the PEG-based isolation methods. Indeed, different isolation methods may lead to the shift or differences in size distributions of the collected EVs, as already evidenced for SEC and UC isolation methods [39,40]. In our case, the PEG-based method is expected to capture non-selectively all EVs subpopulations, leading to more EVs fractions being visualized with CE-LIF as seen in Fig. 6. NTA measurements for both pony serum and plasma revealed a shift towards smaller size distributions when using the droplet approach (Fig. S7 in ESI). This may correspond to an increased concentration of the small-sized subpopulations, which may correlate to the more pronounced appearance of the third peak zone (15–20 min) in the CE-LIF electropherograms. Nevertheless, no further speculation was made to interpret the presence of these three subpopulations observed by CE as no clear relationship between size and charge properties of EVs and their electrophoretic mobilities can be stated at this stage.

## 4. Conclusion remarks

We successfully developed a new approach (instrumentation and methodology) for EVs isolation from both pre-purified standards and biofluid samples, for the first time in microfluidic droplet format. Using a train of micrometric droplets, containing magnetic beads in the first droplet, the sample, washing and elution solutions in the following ones, we allowed significant sample and reagent volume reduction (by 5 times), minimization of manual operations, diminution of operation time (by twice) and improvement of EVs recovery rate by almost 2 folds. Thanks to automatization and miniaturization that we achieved with droplet microfluidics higher throughput can now be expected. Integration of this microfluidic EVs isolation module as a forefront of downstream EVs analysis and characterization is now envisioned. In the present proof-of-concept study that deals with both instrumental and methodological developments at the same time, the univariate approach was chosen to better understand the impact of the different experimental factors. Indeed, the study on EVs is still at early and emerging stage, and all parameters that would have influence on the EVs stability and behaviour (e.g., morphology modification, surface charge changes, risk of lysis etc.) have not been all identified and mastered, which in turn do not allow simultaneous investigation of multiple variables during the optimization of EVs capture and release. Further optimizations with the multivariate approach could be envisaged in the next phase when all risks of EVs modifications during experiments could be mastered and understood.

## Author statement

**Marco Morani:** Methodology, Validation, Investigation, Writing –

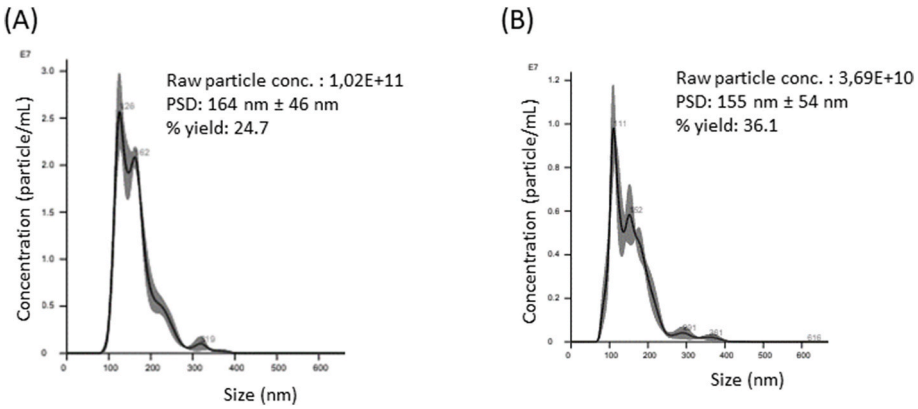


**Fig. 5.** NTA measurements of EVs-spiked artificial serum before (A) and after (B) EVs isolation using the microfluidic droplet platform. The sample was 5-time diluted with PBS prior to microfluidic droplet operations. NTA histograms represent the mean of three replicate measurements of the same sample, with the standard deviation (SD) in grey.

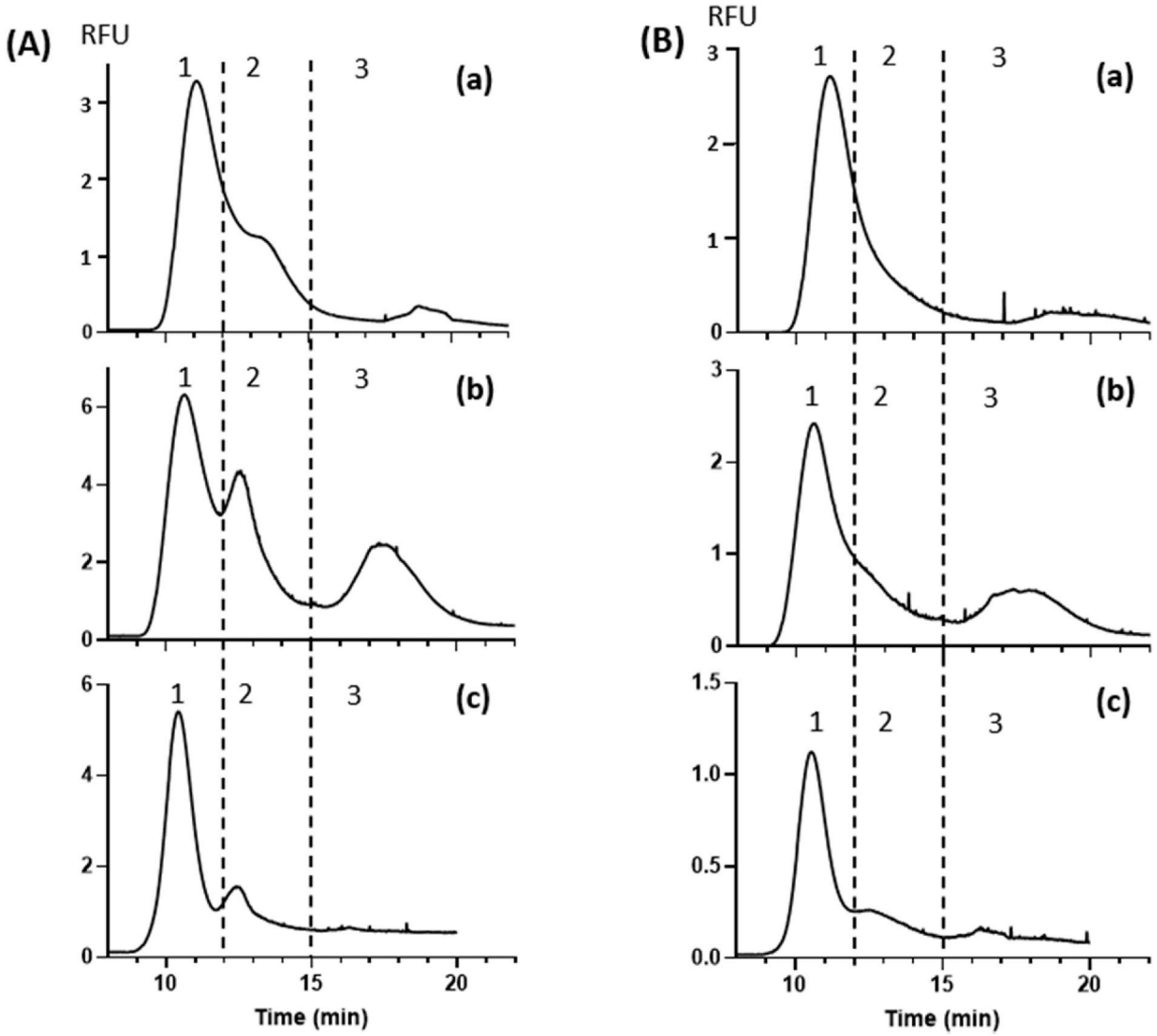


**Fig. 6.** CE-LIF for EVs from pony plasma (A) and serum (B), isolated with PEG-based EVs precipitation method in batch mode (a); with the microfluidic droplet system using the U-shaped pattern (b) and isolated with SEC (c). CE conditions as in Fig. 2.

original draft. **Myriam Taverna:** Funding acquisition; Investigation; Methodology; Supervision; Writing – review & editing. **Zuzana Krupova:** Resources; Methodology, Validation. **Pierre Defrenaix:** Resources; Methodology, Validation. **Lucile Alexandre:** Investigation, Methodology. **Thanh Duc Mai:** Project administration, Funding acquisition, Supervision, Writing – original draft, Writing – review & editing.

## Declaration of competing interest

The authors declare that they have no known competing financial interests or personal relationships that could have appeared to influence the work reported in this paper.

## Acknowledgement

This work has been financially supported by the Institut Universitaire de France (for M. Taverna, senior member) and the Agence Nationale de la Recherche (ANR, France) with the grant no. ANR-18-CE29-0005-01. This project has received funding from the European Union's Horizon 2020 research and innovation programm under the marie Skolodowska-Curie grant agreemrnt No 896313. The doctoral scholarship for Marco Morani was supported by the doctoral school 2MIB (Sciences Chimiques: Molécules, Matériaux, Instrumentation et Biosystèmes) – University Paris Saclay.

## Appendix A. Supplementary data

Supplementary data to this article can be found online at https://doi.org/10.1016/j.talanta.2022.123625.

## References

[1] G. van Niel, G. D'Angelo, G. Raposo, Shedding light on the cell biology of extracellular vesicles, Nat. Rev. Mol. Cell Biol. 19 (4) (2018) 213–228.
[2] L.M. Doyle, M.Z. Wang, Overview of extracellular vesicles, their origin, composition, purpose, and methods for exosome isolation and analysis, Cells 8 (7) (2019) 24.
[3] J. Howitt, A.F. Hill, Exosomes in the pathology of neurodegenerative diseases, J. Biol. Chem. 291 (52) (2016) 26589–26597.
[4] W. Guo, Y.B. Gao, N. Li, F. Shao, C.N. Wang, P. Wang, Z.L. Yang, R.D. Li, J. He, Exosomes: new players in cancer, Oncol. Rep. 38 (2) (2017) 665–675.
[5] P. Vader, E.A. Mol, G. Pasterkamp, R.M. Schiffelers, Extracellular vesicles for drug delivery, Adv. Drug Deliv. Rev. 106 (2016) 148–156.
[6] H.C. Bu, D.G. He, X.X. He, K.M. Wang, Exosomes: isolation, analysis, and applications in cancer detection and therapy, Chembiochem 20 (4) (2019) 451–461.
[7] Z. Zhao, H. Wijerathne, A.K. Godwin, S.A. Soper, Isolation and analysis methods of extracellular vesicles (EVs), Extracell. Vesic. Circ. Nucl. Acids 2 (1) (2021) 80–103.
[8] C. Gardiner, D. Di Vizio, S. Sahoo, C. Thery, K.W. Witwer, M. Wauben, A.F. Hill, Techniques used for the isolation and characterization of extracellular vesicles: results of a worldwide survey, J. Extracell. Vesicles 5 (2016).
[9] M.Y. Konoshenko, E.A. Lekchnov, A.V. Vlassov, P.P. Laktionov, Isolation of extracellular vesicles: general methodologies and latest trends, BioMed Res. Int. (2018) 27.
[10] H. Yan, Y. Li, S. Cheng, Y. Zeng, Advances in analytical technologies for extracellular vesicles, Anal. Chem. 93 (11) (2021) 4739–4774.
[11] T. Liangsupree, E. Multia, M.-L. Riekkola, Modern isolation and separation techniques for extracellular vesicles, J. Chromatogr. A 1636 (2021), 461773.
[12] M. Morani, T.D. Mai, Z. Krupova, G. van Niel, P. Defrenaix, M. Taverna, Recent electrokinetic strategies for isolation, enrichment and separation of extracellular vesicles, TrAC Trends Anal. Chem. (Reference Ed.) (2021), 116179.
[13] S. Hassanpour Tamrin, A. Sanati Nezhad, A. Sen, Label-free isolation of exosomes using microfluidic technologies, ACS Nano 17047-17079 (2021).
[14] Y. Meng, M. Asghari, M.K. Aslan, A. Yilmaz, B. Mateescu, S. Stavrakis, A. J. deMello, Microfluidics for extracellular vesicle separation and mimetic synthesis: recent advances and future perspectives, Chem. Eng. J. 404 (2021), 126110.
[15] D. Yang, W. Zhang, H. Zhang, F. Zhang, L. Chen, L. Ma, L.M. Larcher, S. Chen, N. Liu, Q. Zhao, P.H.L. Tran, C. Chen, R.N. Veedu, T. Wang, Progress, opportunity, and perspective on exosome isolation - efforts for efficient exosome-based theranostics, Theranostics 10 (8) (2020) 3684–3707.
[16] W.T. Su, H.J. Li, W.W. Chen, J.H. Qin, Microfluidic strategies for label-free exosomes isolation and analysis, TrAC Trends Anal. Chem. (Reference Ed.) 118 (2019) 686–698.
[17] S.J. Lin, Z.X. Yu, D. Chen, Z.G. Wang, J.M. Miao, Q.C. Li, D.Y. Zhang, J. Song, D. X. Cui, Progress in microfluidics-based exosome separation and detection technologies for diagnostic applications, Small 16 (9) (2020).
[18] M. Garcia-Contreras, S.H. Shah, A. Tamayo, P.D. Robbins, R.B. Golberg, A. J. Mendez, C. Ricordi, Plasma-derived exosome characterization reveals a distinct microRNA signature in long duration Type 1 diabetes, Sci. Rep. 7 (2017) 10.
[19] M.N. Madison, J.L. Welch, C.M. Okeoma, Isolation of exosomes from semen for in vitro uptake and HIV-1 infection assays, Bio-Protocol 7 (7) (2017) 21.
[20] C. Campos-Silva, H. Suárez, R. Jara-Acevedo, E. Linares-Espinós, L. Martinez-Piñeiro, M. Yáñez-Mó, M. Valés-Gómez, High sensitivity detection of extracellular vesicles immune-captured from urine by conventional flow cytometry, Sci. Rep. 9 (1) (2019) 1–12.
[21] H. Kim, S. Shin, ExoCAS-2: rapid and pure isolation of exosomes by anionic exchange using magnetic beads, Biomedicines 9 (1) (2021) 12.
[22] X. Fang, C. Chen, B. Liu, Z. Ma, F. Hu, H. Li, H. Gu, H. Xu, A magnetic bead-mediated selective adsorption strategy for extracellular vesicle separation and purification, Acta Biomater. 336-347 (2021).
[23] K. Zhang, Y. Yue, S. Wu, W. Liu, J. Shi, Z. Zhang, Rapid capture and nondestructive release of extracellular vesicles using aptamer-based magnetic isolation, ACS Sens. 4 (5) (2019) 1245–1251.
[24] D. Brambilla, L. Sola, A.M. Ferretti, E. Chiodi, N. Zarovni, D. Fortunato, M. Criscuoli, V. Dolo, I. Giusti, V. Murdica, EV separation: release of intact extracellular vesicles immunocaptured on magnetic particles, Anal. Chem. 93 (13) (2021) 5476–5483.
[25] C. Liu, X. Xu, B. Li, B. Situ, W. Pan, Y. Hu, T. An, S. Yao, L. Zheng, Single-exosome-counting immunoassays for cancer diagnostics, Nano Lett. 18 (7) (2018) 4226–4232.
[26] J. Ko, Y. Wang, K. Sheng, D.A. Weitz, R. Weissleder, Sequencing-based protein analysis of single extracellular vesicles, ACS Nano 15 (3) (2021) 5631–5638.
[27] T.D. Mai, D. Ferraro, N. Aboud, R. Renault, M. Serra, N.T. Tran, J.-L. Viovy, C. Smadja, S. Descroix, M. Taverna, Single-step immunoassays and microfluidic droplet operation: towards a versatile approach for detection of amyloid-beta peptide-based biomarkers of Alzheimer's disease, Sens. Actuators, B 255 (2018) 2126–2135.
[28] M. Morani, T.D. Mai, Z. Krupova, P. Defrenaix, E. Multia, M.-L. Riekkola, M. Taverna, Electrokinetic characterization of extracellular vesicles with capillary electrophoresis: a new tool for their identification and quantification, Anal. Chim. Acta 1128: 42-51 (2020).
[29] D. Volodkin, V. Ball, P. Schaaf, J.C. Voegel, H. Mohwald, Complexation of phosphocholine liposomes with polylysine: stabilization by surface coverage versus aggregation, Biochim. Biophys. Acta Biomembr. 1768 (2) (2007) 280–290.
[30] D. Volodkin, H. Mohwald, J.C. Voegel, V. Ball, Coating of negatively charged liposomes by polylysine: drug release study, J. Contr. Release 117 (1) (2007) 111–120.
[31] Y. Takechi, H. Tanaka, H. Kitayama, H. Yoshii, M. Tanaka, H. Saito, Comparative study on the interaction of cell-penetrating polycationic polymers with lipid membranes, Chem. Phys. Lipids 165 (1) (2012) 51–58.
[32] A. Gorman, K.R. Hossain, F. Cornelius, R.J. Clarke, Penetration of phospholipid membranes by poly-L-lysine depends on cholesterol and phospholipid composition, Biochim. Biophys. Acta Biomembr. 1862 (2) (2020) 10.
[33] A. Ali-Cherif, S. Begolo, S. Descroix, J.-L. Viovy, L. Malaquin, Programmable magnetic tweezers and droplet microfluidic device for high-throughput nanoliter multi-step assays, Angew. Chem. Int. Ed. 51 (43) (2012) 10765–10769.
[34] U. Gündüz, Viscosity prediction of polyethylene glycol–dextran–water solutions used in aqueous two-phase systems, J. Chromatogr. B 743 (1–2) (2000) 181–185.
[35] M.A. Stremler, F.R. Haselton, H. Aref, Designing for chaos: applications of chaotic advection at the microscale, Philos. Trans. R. Soc. A-Math. Phys. Eng. Sci. 362 (1818) 1019–1036, 2004.
[36] D. Bedding, C. Hidrovo, Asme, Investigation of Mixing in Colliding Droplets Generated in Flow-Focusing Configurations Using Laser Induced Fluorescence, Amer. Soc. Mechanical Engineers, New York, 2016.
[37] D. Bachurski, M. Schuldner, P.H. Nguyen, A. Malz, K.S. Reiners, P.C. Grenzi, F. Babatz, A.C. Schauss, H.P. Hansen, M. Hallek, E.P. von Strandmann, Extracellular vesicle measurements with nanoparticle tracking analysis - an accuracy and repeatability comparison between NanoSight NS300 and ZetaView, ? J. Extracell. Vesic. 8 (1) (2019).
[38] J.A. Jaros, P.C. Guest, S. Bahn, D. Martins-de-Souza, Affinity Depletion of Plasma and Serum for Mass Spectrometry-Based Proteome Analysis, Proteomics for Biomarker Discovery, Springer, 2013, pp. 1–11.
[39] K. Takov, D.M. Yellon, S.M. Davidson, Comparison of small extracellular vesicles isolated from plasma by ultracentrifugation or size-exclusion chromatography: yield, purity and functional potential, J. Extracell. Vesicles 8 (1) (2019), 1560809.
[40] K. Brennan, K. Martin, S. FitzGerald, J. O'Sullivan, Y. Wu, A. Blanco, C. Richardson, M. Mc Gee, A comparison of methods for the isolation and separation of extracellular vesicles from protein and lipid particles in human serum, Sci. Rep. 10 (1) (2020) 1–13.